Scientific Research Publishing

World Journal of Mechanics, 2022, 12, 41-50
https://www.scirp.org/journal/wjm
ISSN Online: 2160-0503
ISSN Print: 2160-049X

Experimental Study on Vortex Growth during the Early Development of Rotating Disks

Hiroyuki Furukawa, Takeomi Yamazaki

Department of Mechanical Engineering, Meijo University, Nagoya, Japan
Email: furukawa@meijo-u.ac.jp

How to cite this paper: Furukawa, H. and Yamazaki, T. (2022) Experimental Study on Vortex Growth during the Early Development of Rotating Disks. *World Journal of Mechanics*, **12**, 41-50.
https://doi.org/10.4236/wjm.2022.123003

Received: March 12, 2022
Accepted: March 28, 2022
Published: March 31, 2022

Abstract

In previous studies, the effects of radial clearance on the flow of a rotating disk in a cylindrical vessel have been investigated by using rotating disks of different shapes. As a result, different flow phases were observed in each disk due to the difference in disk dimensions. In this study, we focus on the end-face effect and conduct experiments to visualize the vortex growth process and elucidate the generation mechanism of the vortex structure. From the experiment results, at Re = 4000, 7000, and 9000, four types of vortex flow modes appeared in the vortex development process. However, at Re = 4000, only regular 2-cells and regular 4-cells appeared, and at Re = 9000, only mutated 2-cells and mutated 3-cells appeared. In addition, it was found that only one type appeared depending on the rotational ascent time t_s. When Re = 4000, the rotational ascent time t_s = 0, 2, 7, and 8 was stable at regular 4-cells, while the others were finally stable in regular 2-cells. This study revealed the influence of the acceleration of the rotating disk on the non-unique flows in the cylindrical casing.

Keywords

Rotating Disk, Experimental Study, Flow Instability, Non-Uniqueness

1. Introduction

From long ago, numerous studies have been undertaken on the flow induced by a rotating object in a vessel, as has been seen in fluid machinery such as centrifugal pumps and water wheels, and where energy is transferred to and from the fluid by the rotation of an impeller; such studies were performed by Bödewadt [1] and others. If there is a large gap between both disks, the flow has a separating boundary layer, and this case was studied by Batchelor [2]. Other studies investigated the flow around the eccentric rotating porous disks [3] or the nonli-

near vortex structures in obliquely rotating fluid [4].

However, in many previous studies, the rotating disk has only been used to give a circumferential velocity component, with little consideration given to the shape of the disk. However, it is known that the radial gap greatly affects the flow between the fixed and rotating disks at the bottom of the vessel [5]. The effect of this radial gap on the flow between the bottom of the vessel and the rotating disk [6] is called the end-face effect.

In previous studies, the effects of radial clearance on the flow of a rotating disk in a cylindrical vessel have been investigated by using rotating disks of different shapes. As a result, different flow phases were observed in each disk due to the difference in disk dimensions. In this study, we focus on the end-face effect and conduct experiments to visualize the vortex growth process and elucidate the generation mechanism of the vortex structure. In this study, we investigated experimentally the influence of the acceleration of the rotating disk on the vortex growth during the early development of rotating disks.

2. Experimental Apparatus

2.1. Main Parts of the Experimental Apparatus

Figure 1 shows the main part of the experimental apparatus. The cylindrical vessel containing the test fluid consists of two fixed disks (top and bottom) and a cylindrical frame with an inner diameter of 142.0 mm and a thickness of 40.0 mm sandwiched between the same disks. Both the fixed disk and cylindrical frame are made of acrylic resin. The rotating disk is mounted on a rotating shaft with a shaft diameter of 20.0 mm. In the inter-disk flow, which is the flow pattern between the rotating disk and fixed disk, the disk joint is 20.0 mm in diameter, which is the same as the axis of rotation, to make the space inside the vessel symmetrical across the rotating disk.

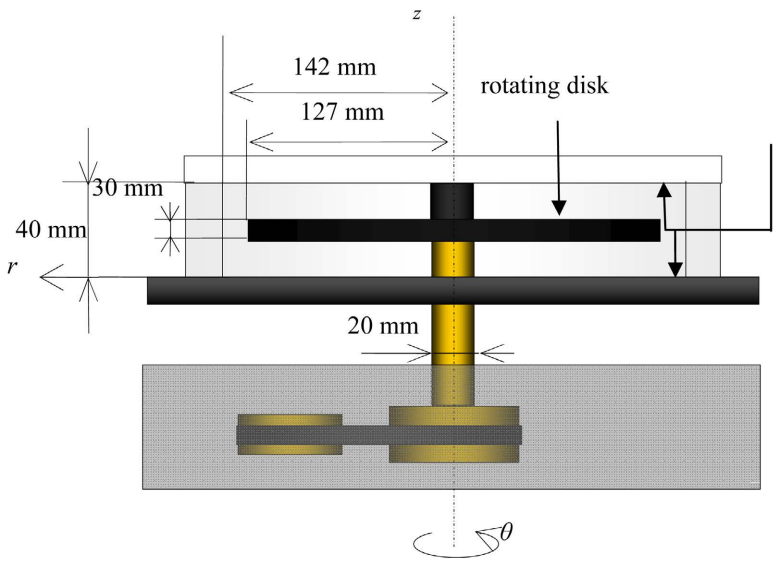

Figure 1. Points at which axial velocity is analyzed.

2.2. Rotating Disks

The dimensions of the rotating disk to be installed inside the vessel are as follows.

Disk F: radius r_d = 127.0 mm, thickness h_d = 30.0 mm

The disk is made of duralumin, and the entirety of the disk is painted in matte black.

2.3. Experimental Apparatus and Peripherals

The experimental apparatus consists of an acrylic casing (Sanwa Kikai Seisakusho), a xenon light source (XENON-ARC SRX-80A, Kato Koken Co., Ltd.), an inverter (Mitsubishi Electric Corporation), a control box (Sanwa Kikai Seisakusho), a digital tachometer (Mitsubishi Electric Corporation), and the main part of the experimental apparatus attached before it. There is a single-lens reflex camera (EOS Kiss X3, Canon) with a frame rate of 30 fps and a resolution of 1280 × 720 pixels. In this study, a lens (B016, TAMRON) with a focal length of 16 - 300 mm is attached to a single-lens reflex camera, and this is used for shooting. The video files are imported into a PC, and PIV analysis software (Koncerto, Seika Corporation.) is used to perform PIV analysis.

The light source is placed directly beside the cylindrical vessel such that the irradiation position is horizontal, and the experimental apparatus is located in the darkroom to block the light from the outside. In addition, the motor has been replaced by a stepless conversion motor to obtain the required rotational speed. The rotational speed of the motor is controlled by an inverter, the disk acceleration time is set by MELSOFT series GX Works II (Mitsubishi Electric), and the shaft speed is checked by a digital tachometer.

3. Experimental Method

3.1. Preparation of Test Fluids

A mixture consisting of distilled water and aluminum powder mixed in a given ratio is used as the test fluid. In order to obtain the kinematic viscosity ν of the test fluid, the specific gravity s was examined using a specific gravity meter (Japan Measuring Instruments, K.K.). Additionally, viscosity μ is measured using an SV-type viscometer (SV-10, A & D Co., Ltd.).

3.2. Visualization Method

The three-dimensional flow in the vessel is visualized in a two-dimensional plane by using aluminum powder and a slit.

When this test fluid is injected into a vessel and irradiated with a xenon light source, the flow can be visualized and observed. The light source is captured through the application of a slit that enables observation of the r-z cross-section.

In addition, 1 - 2 drops of a neutral household detergent are mixed to prevent the aluminum powder from floating due to the surface tension of the test fluid.

3.3. Visualization Part

The part to be visualized is the plane r-z section created by the radial r-axis and axial z-axis of the disk.

3.4. Reynolds Number

Reynolds number = $\omega r_d^2 / \nu$ is used as the index of flow. ω is the angular velocity of the rotating disk, which is calculated from the number of disk rotations N. All rotating disks rotate counter-clockwise.

For the disk rotation speed, set the disk ascent time t_s (s) and increase the speed from the initial stationary state to the rotation speed corresponding to the desired Reynolds number based on the set time. Then, after the target rotational speed is reached, t_s = 1 s. On this occasion, a disk of 30 mm is used. The Reynolds number is tested in increments of 1000 from 3000 to 10,000, and the rotational ascent time ranges from 0 (s) to 10 (s).

4. Experimental Results

4.1. Development Process at Reynolds Number of 4000

In Figure 2, the regular 4-cell vortex developed 13 (s) after the start of the rotation, and then remained stable. This development process was observed with a rotational ascent time of 0 (s) to 2 (s).

In Figure 3, the regular 4-cell vortex developed 35 (s) after the start of the rotation, but at 70 (s) the upper and lower outer vortices swallow the inner vortex and change to a regular 2-cell vortex at 110 (s), which stabilizes. This development process was observed in the rotational ascent time range of 3 (s) to 10 (s).

Figure 4 shows a graph of mode discrimination from 20 (s), when the mode could be discriminated at a Reynolds number of 4000 and rotational ascent time t_s = 0 - 10, to 120 (s), when the mode stabilized.

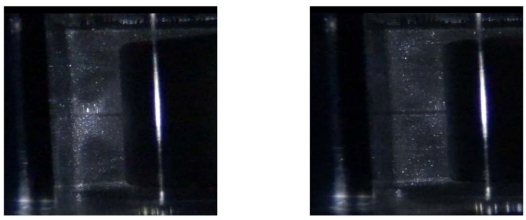

Figure 2. Re = 4000, t_s = 2.

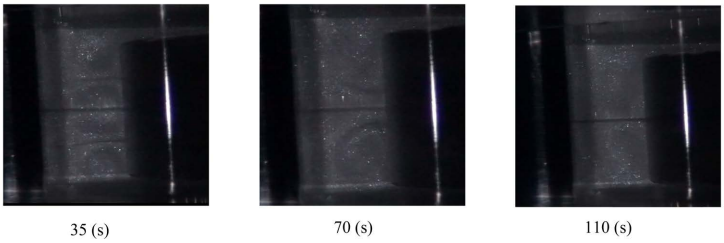

Figure 3. Re = 4000, t_s = 3.

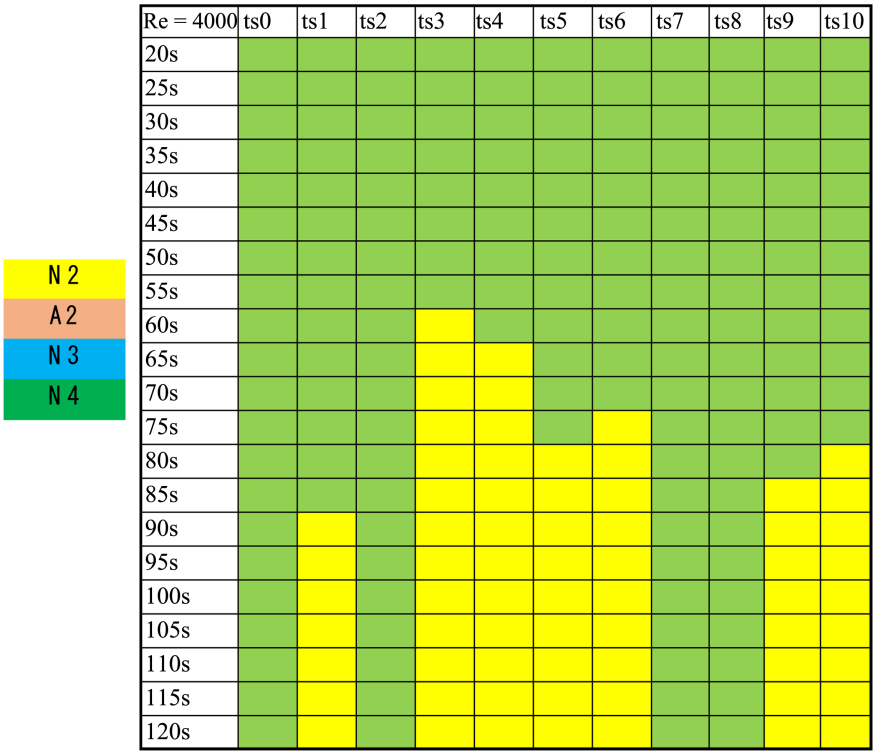

Figure 4. Flow mode (Re = 4000).

4.2. Development Process at Reynolds Number of 7000

Figure 5 shows a mutated 2-cell vortex developed 30 (s) after the start of the rotation. Following this, at 40 (s), a vortex developed from the lower part of the disk and developed into a mutant 3-cell, but soon changed to a mutated 2-cell. The same change was observed at 55 (s) and 85 (s), and this was characterized by the fact that the time to maintain the mutated 3-cell increased as time passed from the start of the rotation. This development process was also observed in the change between the regular 4-cell and mutated 3-cell with a rotational ascent time of $t_s = 6$.

In Figure 6, the cell developed into a mutated 3-cell after the start of the rotation, and then changed to a regular 4-cell at 40 (s); however, soon after that, a vortex developed from the top of the disk and changed to a mutated 3-cell. Furthermore, if we look at Figure 8, the same change can be seen repeatedly, with a lengthening of the maintenance of the mutated 3-cell (s). In Figure 7, the vortex developed from the top of the disk at 20 (s) from the start of the rotation, and this resulted in a mutated 3-cell vortex. At 85 (s), the cell changed to a regular 2-cell, and at 100 (s), a vortex developed from the top of the disk and changed to a mutated 3-cell. Again, if we look at Figure 8, we can see that similar changes are repeated.

Figure 8 shows a graph of mode discrimination from 20 (s), when the mode could be discriminated at a Reynolds number of 7000 and rotational ascent time $t_s = 0$ - 10, to 120 (s), when the mode stabilized.

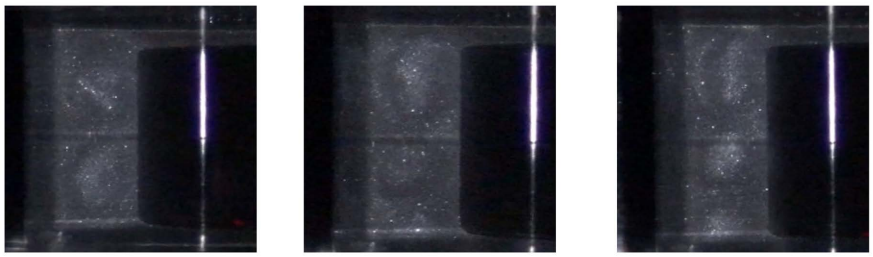

Figure 5. Re = 7000, t_s = 0.

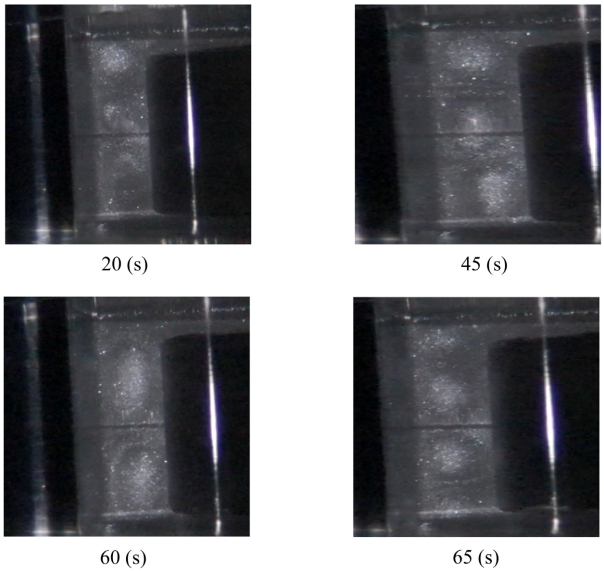

Figure 6. Re = 7000, t_s = 4.

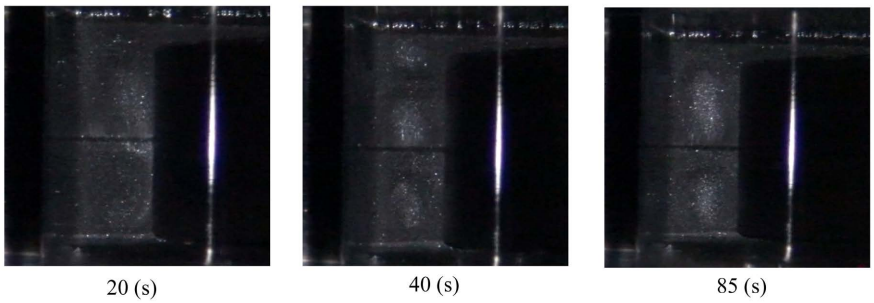

Figure 7. Re = 7000, t_s = 8.

4.3. Development Process at Reynolds Number of 9000

In Figure 9, a mutated 2-cell vortex developed and remained stable. This development process was observed at rotational ascent times of 0 (s) to 2 (s), 4 (s), and 5 (s).

In Figure 10, a mutated 2-cell develops immediately after the start of rotation, and this then changed to repeat regular 3-cell and mutated 2-cell. This was only observed at a rotational ascent time of 3 (s). On the left side of Figure 11, a mutated 2-cell developed immediately after the start of rotation, but this temporarily

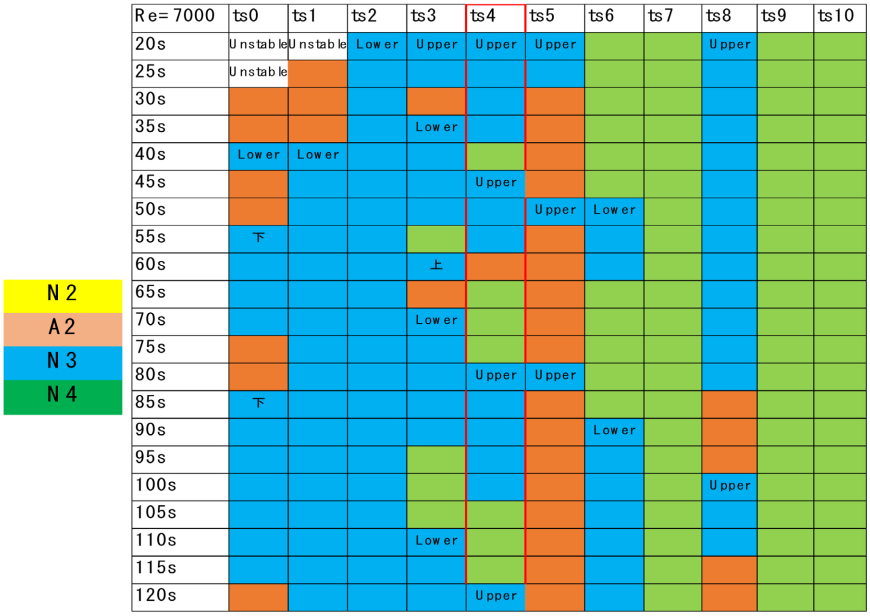

Figure 8. Flow mode (Re = 7000, Upper: Developed from upper end wall, Lower: Developed from lower end wall).

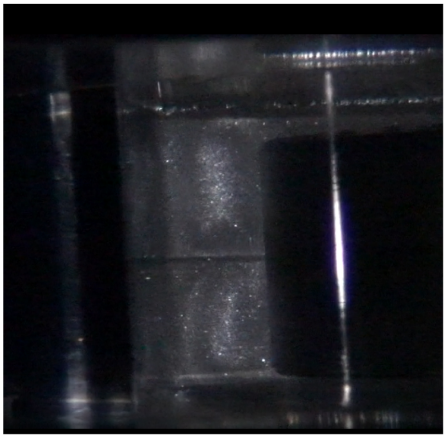

Figure 9. Re = 9000, t_s = 2.

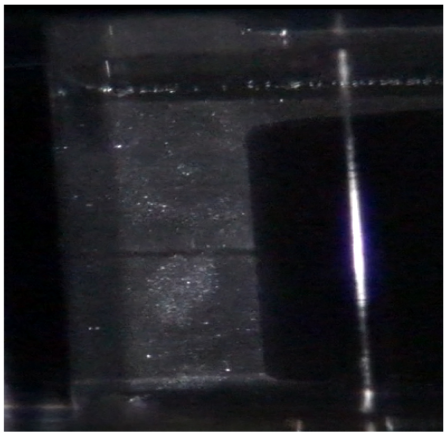

Figure 10. Re = 9000, t_s = 3.

changed to a regular 3-cell as a vortex developed from the lower part of the disk. After that, it stabilized in the mutated 2-cell. Similarly, on the right side of Figure 11, however, a mutated 2-cell developed immediately after the start of rotation, but temporarily changed to a regular 3-cell as a vortex developed from the top of the disk. A difference was seen in the development of a regular 3-cell vortex from the bottom of the disk at the rotational ascent time of 6 (s), and from the top of the disk at the rotational ascent times of 7 (s) and 8 (s).

In Figure 12, regular 3-cell vortices developed and remained stable. This development process was observed for a rotational ascent time of 9 (s) and 10 (s).

Figure 13 shows a graph of mode discrimination at Reynolds number 9000 with rotational ascent time of t_s = 0 - 10.

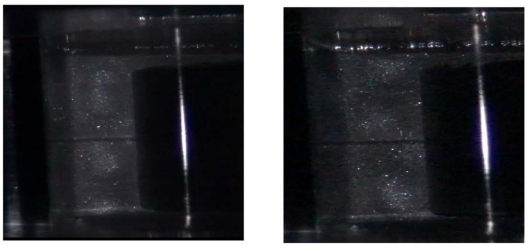

Figure 11. Re = 9000, Left: t_s = 6, Right: t_s = 8.

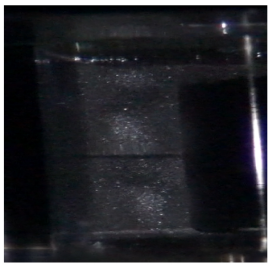

Figure 12. Re = 7000, t_s = 9.

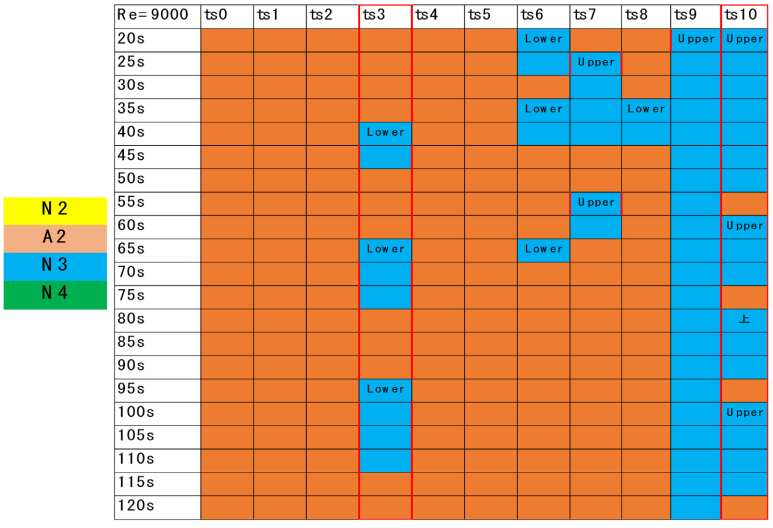

Figure 13. Flow mode (Re = 9000, Upper: Developed from upper end wall, Lower: Developed from lower end wall).

5. Conclusions

In previous study, the flows around the rotating disk are classified by just the Reynolds number. This study investigated the influence of the acceleration of the rotating disk, and the non-uniqueness flows appear according to the acceleration time of the rotating disks.

From the experiment results, at Re = 4000, 7000, and 9000, four types of vortex flow modes appeared in the vortex development process. However, at Re = 4000, only regular 2-cells and regular 4-cells appeared, and at Re = 9000, only mutated 2-cells and mutated 3-cells appeared. In addition, it was found that only one type appeared depending on the rotational ascent time t_s.

When Re = 4000, the rotational ascent time t_s = 0, 2, 7, and 8 was stable at regular 4-cells, while the others were finally stable in regular 2-cells.

In cases where Re = 7000, when the rotational ascent time t_s = 0, 4, and 6, the variation of mutated 3-cells is repeated periodically, and the longer the time elapsed from the start time, the longer the mutated 3-cell was maintained. At a rotational ascent time of t_s = 3, the vortex of the mutated 3-cells temporarily developed from the upper part of the rotating disk; however, the vortex of mutated 3-cells changed periodically from the lower part of the rotating disk. When the rotational ascent time t_s = 5, the vortex of mutated 3-cells develops periodically from the upper part of the rotating disk; however, it immediately changes to regular 2-cells. At a rotational ascent time of t_s = 8, mutated 3-cells were repeated from the start of rotation to 85 (s), at which point the mutated 2-cells and mutated 3-cells repeatedly changed. At rotational ascent times of t_s = 1 and 2, the mutated 3-cells finally stabilize, and at t_s = 7, 9 and 10, the regular 4-cells stabilize.

In the case of Re = 9000, the vortex developed from the lower part of the disk at the rotational ascent time t_s = 3, 6, and in the case of t_s = 7, 8, 9 and 10, the vortex was seen to develop from the upper part. The result was such that the mutated 3-cells remained stable only when the rotational ascent time t_s = 9. It can be seen that the duration of the development of the mutated 3-cells increases by 5 (s) with each iteration from the regular 2-cells with a rotational ascent time of t_s = 3.

When the Reynolds number is small, the influence of the acceleration of the rotating disk is not so large, but under high Reynolds number, the influence is larger. In our future work, we will investigate the influence of the acceleration rate of the rotating disk at different sizes of the rotating disks.

Acknowledgements

We would like to show our gratitude to members in our laboratory for sharing their pearls of wisdom with us during the course of this research, and we thank "anonymous" reviewers for helpful comments that greatly improved the manuscript.

Conflicts of Interest

The authors declare no conflicts of interest regarding the publication of this paper.

References

[1] Bödewadt, U.T. (1940) Rotary Currents on Fixed Grounds. *Zeitschrift fur Angewandte Mathematik und Mechanik*, **20**, 241-253. https://doi.org/10.1002/zamm.19400200502

[2] Batchelor, G.K. (1951) Note on a Class of Solutions of the Navier-Stokes Equations Representing Steady Rotationally Symmetric Flow. *Quarterly Journal of Mechanics and Applied Mathematics*, **4**, 29-41. https://doi.org/10.1093/qjmam/4.1.29

[3] Ersoy, H. (2018) Flow of a Second-Grade Fluid between Eccentric Rotating Porous Disks in the Presence of a Magnetic Field. *Open Journal of Applied Sciences*, **8**, 159-169. https://doi.org/10.4236/ojapps.2018.85013

[4] Kopp, M., Tur, A. and Yanovsky, V. (2015) Nonlinear Vortex Structures in Obliquely Rotating Fluid. *Open Journal of Fluid Dynamics*, **5**, 311-321. https://doi.org/10.4236/ojfd.2015.54032

[5] Serre, E., Del Arco, E.C. and Bontoux, P. (2001) Annular and Spiral Patterns in Flows between Rotating and Stationary Disk. *Journal of Fluid Mechanics,* **434**, 65-68. https://doi.org/10.1017/S0022112001003494

[6] Jeong, J. and Hussain, F. (1995) On the Identification of a Vortex. *Journal of Fluid Mechanics,* **285**, 69-94. https://doi.org/10.1017/S0022112095000462